Repair of Corrosion-Damaged Columns with FRP Wraps

By S. J. Pantazopoulou,[1] J. F. Bonacci,[2] S. Sheikh,[3] Members, ASCE,
M. D. A. Thomas,[4] and N. Hearn[5]

Abstract: Corrosion of reinforcement in bridge piers is encouraged by chloride contamination from exposure to marine environment and from deicing salts used in bridges during winter. Because corrosion products generally occupy greater volume than the original material, expansive forces are generated in concrete leading to spalling of the cover and further acceleration of the reinforcement disintegration. Jacketing of such structures by fiber-reinforced composite sheets is an effective remedy, not only as a means of slowing down the rate of the reaction, but also by confining the concrete core thereby imparting to it ductility and strength. This paper presents results of an experimental parametric study of this method as a repair alternative for corroded structures. Several small-size concrete columns with various reinforcement configurations were subjected to accelerated corrosion conditions in the laboratory. After a target level of steel loss was attained the columns were repaired using a variety of repair alternatives. Most of the repair schemes considered included jacketing the damaged specimens with glass-fiber wraps, in combination with grouting the voids between the jacket and the original lateral surface of the specimen with either conventional or expansive grouts. To protect the glass fiber material from exposure to alkali activity of the fresh grout, and to reduce the supply of oxygen and water to the mechanism of corrosion, different types of diffusion barriers were considered in the study. The efficacy of each repair system was evaluated by (1) assessing the postrepair corrosion resistance of the specimens under repeated exposure to accelerated conditions; and (2) the mechanical strength and ductility enhancement under concentric compression loading.

INTRODUCTION

Fiber-reinforced composite sheets are ideal products to be used as jacketing systems for underdesigned or damaged reinforced concrete columns that could benefit from confinement of the concrete core. This technology has found two different fields of application in repair and strengthening of existing reinforced concrete columns and bridge piers: (1) Repair and upgrading for earthquake resistance; and (2) repair of corrosion-damaged members where the transverse and even the longitudinal reinforcement are no longer dependable. The latter option is an economic, expedient, lightweight, and somewhat more durable alternative to conventional repairs of corrosion symptoms in reinforced concrete, and though tested only recently, it is already in use in many field applications throughout Canada. [The first known application of FRP jacketing for repair of corroded structural members was an experimental study that was done by the authors in the mid-1990s at the University of Toronto (Pantazopoulou et al. 1996; Sheikh et al. 1997).] A large part of that study involved conditioning, repair, and testing of the two series of specimens that are reported in this paper. Since that time extensions to this work have been undertaken by the same as well as by other research teams, confirming the findings of this work (Bonacci et al. 1998). Note that the service life of reinforced concrete bridges exposed either to maritime environment or to harsh climatic conditions (where deicing salts are used regularly through several months over the year) is often limited by premature deterioration of important components, such as piers and decks, due to reinforcement corrosion (Manning 1992). Thus, developing practical and economical methods for expedient and successful repair of these structures so as to recover their structural integrity and prolong their useful life is a key objective of modern bridge engineering.

For reinforced concrete transportation structures (bridges and parking garages) conventional repairs often require partial or complete disruption of traffic because of the need of shoring the members under repair, partial removal of contaminated concrete from damaged areas, occasional sandblasting to remove loose rust from the affected reinforcement, and patching the repaired areas with low-permeability concrete. This is a labor-intensive process, yet many argue that patch repairs of this type are not durable. Note that the newly placed concrete cover in the patched areas begins with minimal or no concentration of chlorides. Nevertheless, experience from field applications indicates that this situation changes rapidly, because a reverse chloride concentration gradient is created between the old concrete (core) and the new cover, the result being patch failure and frequent need for repeat repairs (every few years) in the affected region.

The success of jacketing or other confining systems in conventional concrete is in restraining uncontrolled volume expansion as damage accumulates. Note that volume expansion is a characteristic and essential sign of failure in concrete; the greater its magnitude at a given level of axial compressive strain, the more brittle the failure mode. In recent years, jacketing with fiber-reinforced plastic (FRP) products such as composite wraps in lieu of conventional steel jackets is becoming an increasingly popular method of upgrading bridge piers and columns for seismic resistance (Isley 1992). The wraps are usually oriented so as to develop their tensile resistance in the hoop direction. Because they are several times stronger than steel, if properly anchored they can contain volumetric expansion and induce very large confining stresses to the column core concrete. Other attractive advantages of this repair option are that minimal time and labor are required to implement it.

Because corrosion of reinforcement is also an expansive process, causing a need for increased volume displacement of the surrounding concrete in order to accommodate the accumulating corrosion products, repair by means of external con-

[1]Assoc. Prof., Dept. of Civ. Engrg., Demokritus Univ. of Thrace, Xanthi 67100, Greece. E-mail: voula@demo.cc.duth.gr
[2]Assoc. Prof., Dept. of Civ. Engrg., Univ. of Toronto, Ontario, Canada M5S 1A4. E-mail: bonacci@civ.utoronto.ca
[3]Prof., Dept. of Civ. Engrg., Univ. of Toronto, Ontario, Canada M5S 1A4. E-mail: sheikh@civ.utoronto.ca
[4]Assoc. Prof., Dept. of Civ. Engrg., Univ. of Toronto, Ontario, Canada M5S 1A4. E-mail: thomas@civ.utoronto.ca
[5]Asst. Prof., Dept. of Civ. Engrg., Univ. of Windsor, Ontario, Canada. E-mail: hearn@civ.utoronto.ca

Note. Discussion open until July 1, 2001. To extend the closing date one month, a written request must be filed with the ASCE Manager of Journals. The manuscript for this paper was submitted for review and possible publication on March 15, 1999. This paper is part of the ***Journal of Composites for Construction***, Vol. 5, No. 1, February, 2001. ©ASCE, ISSN 1090-0268/01/0001-0003–0011/$8.00 + $.50 per page. Paper No. 20544.

finement is an obvious remedy. Considering that the factors inducing corrosion may continue to affect the structure past the repair stage, the corrosion-resistant FRP wraps promise a much more durable solution than steel jackets in this application. In this paper the concept of external confinement as the strengthening element of corrosion-damaged columns was explored not only as a remedy for strength recovery, but also as a means of delaying or even arresting the process of corrosion by proper design of the confining system. For this purpose, an experimental parametric study was undertaken at the University of Toronto, involving testing under corrosive environments of a series of small scale cylindrical columns repaired with a variety of alternative options. Apart from two series of conventionally repaired and undamaged control specimens that were included in the experimental series for reference, all the repair methods that were studied combined some form of grouting or patch repair with FRP jacketing. Performance variables used to gauge the efficacy of each repair scheme were (1) the rate of postrepair corrosion after repeat conditioning of the repaired specimens to corrosive environments; and (2) mechanical properties (i.e., strength, ductility, and volumetric expansion) of the repaired specimens under uniaxial compression. The following sections outline the experimental program, including details about accelerated corrosion procedures used in order to induce corrosion damage to the specimens, design, and implementation of the repair schemes and performance results.

SPECIMEN DESIGN AND CONDITIONING

Specimen Preparation

Fifty cylindrical column specimens were cast with dimensions 150 mm in diameter by 300 mm in height and reinforced with three 10M (10M = 10 mm nominal diameter) longitudinal steel bars at 10 mm cover (Fig. 1). The equivalent longitudinal reinforcement area given as a fraction of the gross sectional area of the specimen is $\rho_s = 1.7\%$. This reinforcement ratio is representative of typical bridge pier construction that is commonly used in freeway overpasses throughout southern Ontario; specimen dimensions correspond to 1/6-scale models of the typical prototype pier (Pantazopoulou et al. 1996), whereas few 1/2-scale companion models were also considered in the experimental investigation in order to test the most prominent of the repair alternatives (Michniewicz 1996; Sheikh et al. 1997). The need for a parametric assessment of the repairs, including evaluation of the repeatability of their performance dictated the large number of small scale specimens; larger specimens confirmed the experimental findings of the small-scale specimen investigation. During conditioning to accelerated corrosion, the longitudinal reinforcement was connected to the power supply so as to behave as the anode of the electrochemical corrosion cell (to facilitate the electrical connection the anodic reinforcement was protruding from the top face of the specimens; this length was epoxy coated locally to protect the wires from corrosion). The cathode was provided by an additional 10M bar (epoxy-coated) placed along the centerline of each specimen (Fig. 1). Two different arrangements of transverse reinforcement were used in the experimental study, thus separating the specimens into two series each comprising 25 specimens, referred to herein as S and H, and representing different confining circumstances used in practice—spiral confinement in the S case, and no confinement except for two triangular hoops at the top and bottom to support the longitudinal reinforcement in the H case, as illustrated in Fig. 1. Two different concrete mixes were used in casting the specimens. To encourage concentration of the corrosion activity in the middle part of the specimens, the central 210 mm-long test region was cast with a low-quality concrete mix having a water:cement ratio $w_0 = 0.62$ and a 28-day compressive strength $f'_c = 24$ MPa. (This mix is typical of concrete used 20 years ago in bridge construction; in order to encourage corrosion of steel 2.6% cement by weight in sodium chloride was added to the mix.) The remaining end caps were cast of low permeability dense mix having $w_0 = 0.43$ and $f'_c = 57$ MPa.

Conditioning to Accelerated Corrosion

Reinforcement corrosion occurs in conducive environments when the surface layer of the reinforcement is depassivated either because of carbonation of the cover concrete or from excessive chloride concentration in the concrete pore solution. In bridge structures the primary cause of depassivation is adsorption of chlorides used for deicing. Oxygen is essential to

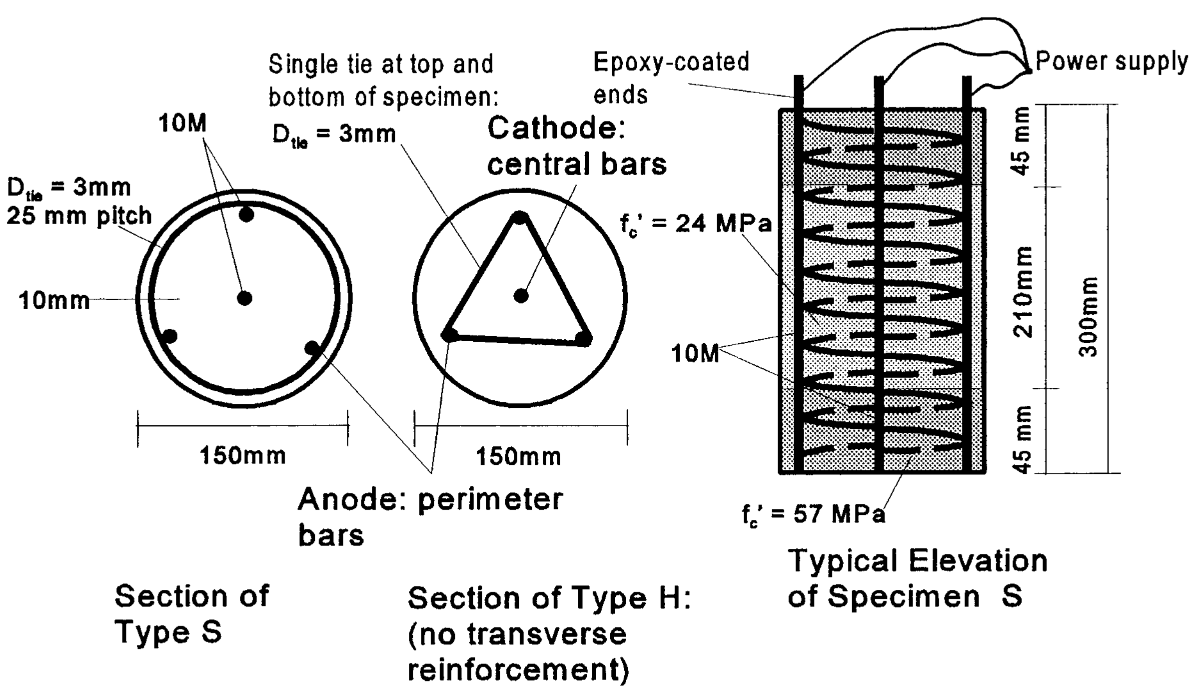

FIG. 1. Typical Specimen Geometry: (a) S-Series; (b) H-Series

sustain the corrosion process which consists of iron dissolution into ferrous oxides (Fe^{2+} ions) and ferric oxides (Fe^{3+} ions) (red rust). Therefore, partially saturated conditions in chloride-contaminated concrete represent the ideal environment to promote the chemical process of corrosion. Under such conditions, corrosion of steel is an expansive process, with the reaction products usually occupying greater volume than the original material. (Under limited oxygen supply the resulting corrosion products are not necessarily expansive, but can be a soft, black, water-soluble compound.) If the corroding steel is embedded in concrete, then the magnitude of tensile stresses generated by the displaced volume of red rust material are high enough to cause cracking and subsequent delamination of the concrete cover.

In conditioning the specimens the objective was to generate similar corrosion products as would occur in nature at an accelerated pace so as to enable systematic study of the corrosion process and product accumulation in a realistic time frame. Accelerating the corrosion was achieved electrochemically by applying a fixed potential of 6 V between the anode (reinforcement cage including transverse steel) and the cathode (central bar) of each specimen (Phillips 1992; Bonacci et al. 1998; Lee 1998). At the initial stages of this phase the specimens were immersed in plastic containers filled to three-fourths of their height in 2% Cl^- solution. After 5 days the solution level was reduced to about 50 mm depth, and the specimens were covered with plastic sheets to maintain a high level of humidity. During the exposure period which lasted about 5 to 6 months, voltage, current, and diametric expansion readings (at midheight and ± 75 mm above and below that section) were taken periodically. Steel loss was calculated from the recorded corrosion current I using Faraday's equation

$$\Delta W\ (\mathrm{g}) = \frac{I \cdot t \cdot A_m}{z \cdot \mathrm{F}} \tag{1}$$

where A_m = atomic mass of the metal (for iron 55.85 g); z = valency [assuming that the rust product is mainly $Fe(OH)_2$, z is taken as 2]; t = time since corrosion initiation (s); and F = Faraday's constant [94,486.7 coulombs (g/equivalent)] (Phillips 1992). [As a point of reference, note that 1 amp hr consumes 1.04 g of iron (Manning 1992).] Representative results are illustrated in Figs. 2 and 3 (as a point of reference, note that the initial mass of anodic reinforcement was 0.95 and 0.73 kg for the typical S and H specimen, respectively). Observed damage in the H series of specimens was more severe than in the S series, most likely because the electrical resistance of the S specimens was greater due to the larger overall amount of reinforcing steel (greater anodic area leading to a lower corrosion current density for a given current). It is also possible that the expansive forces resulting from buildup of corrosion products were partially resisted by the confining action of the spiral reinforcement.

Figs. 2–4 plot time histories of current, steel loss, and radial expansion for representative specimens of the S and H series (specimen numbers 3 and 8 from the S series and specimen numbers 3 and 5 from the H series). Evidently, the total amount of steel loss is in linear relation with the measured radial expansion strain, a finding that supports the basic premise of the proposed repairs, i.e., it appears that mechanical restraint to radial expansion affects the rate of deposition and buildup of corrosion products. Recent tests have investigated the relationship between corrosion damage obtained under accelerated conditions with the naturally occurring corrosion damage under similar exposure conditions (Bonacci et al. 1998; Lee 1998). The results between the two corrosion regimes compare well and confirm the observation that corrosion current is proportional to expansion (due to cover cracking and spalling). It is evident that the more complete the oxidation of the rust products, the more expansive the type of mechanical damage that will result.

REPAIR PROCEDURES

The basic elements of the repair methods tested in this experimental study were

- A layer of dense low-permeability grout overlaid on the damaged concrete
- A diffusion barrier to minimize penetration of moisture and oxygen, and reverse leaching of alkalis from the grout
- Fiber composites wrapped around the repaired specimens,

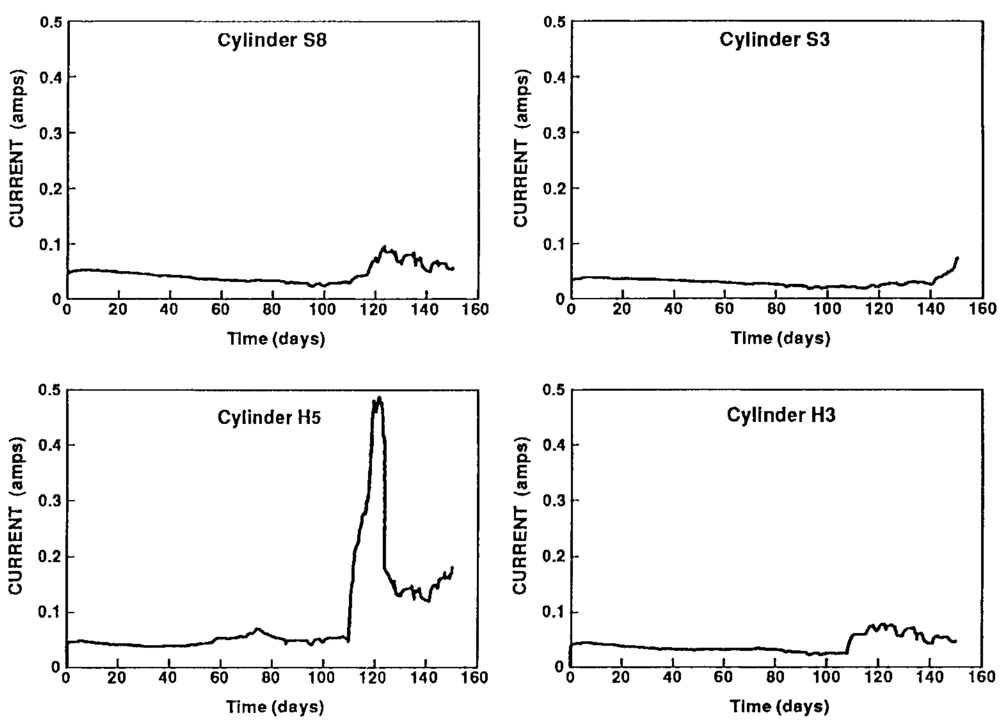

FIG. 2. Variation of Current versus Time of Exposure to Accelerated Corrosion

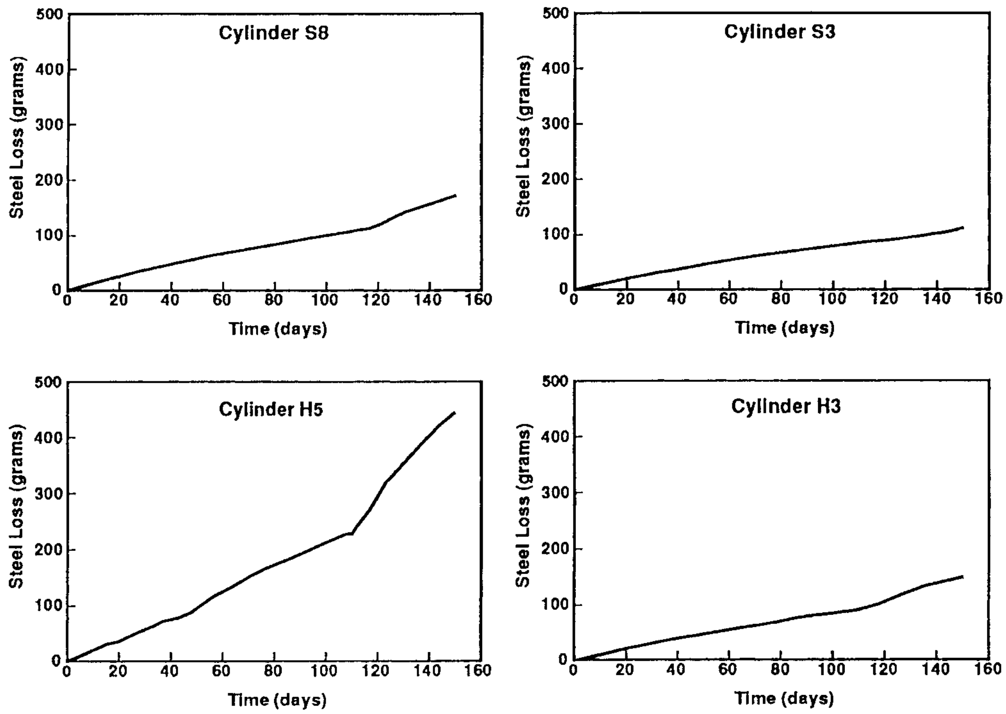

FIG. 3. Estimated Steel Loss versus Time for Representative Samples [Eq. (1)]

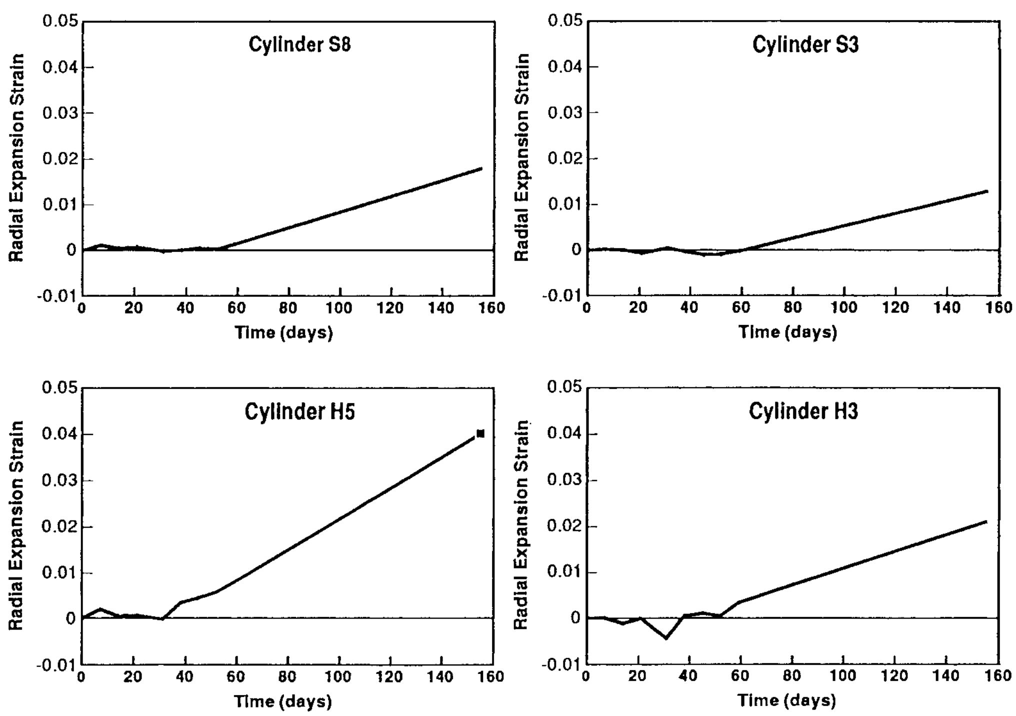

FIG. 4. Measured Radial Expansion due to Reinforcement Corrosion

to induce passive confining stresses in response to future expansion of the encased concrete

Other considerations motivating the design of the repair options were to minimize labor costs by eliminating any work phases that require concrete removal from damaged areas or shoring, and to ensure that mechanical strength and deformability of the members are not compromised by the choice not to remove or replace loose concrete. It was rather anticipated that the losses in the mechanical properties resulting from the existing damage of concrete would be more than offset by the presence of confinement.

Seven different types of repair were considered for specimen series S. To minimize variability due to experimental scatter, three identical specimens were repaired with each repair option except for Option 1 below, which was applied to two specimens only.

Option 1 is conventional repair (removal of the damaged concrete cover and replacement by a patch of low permeability). The steel that was revealed was in very poor condition, brittle, and of drastically reduced diameter (particularly so for the spiral reinforcement). The replacement grout was a silica fume-based, shrinkage compensating compound, reinforced with short polypropylene fibers (trade name EMACO). The

TABLE 1. Summary of Specimen Repairs and Measured Postrepair Performance

Specimen (1)	Repair details (2)	Diameter (mm) (3)	Steel loss[a] (g) (4)	Radial strain (×1,000) (5)	Load (kN) (6)	Stress[c] (MPa) (7)	ε_{peak} (8)	ε_{80} (×1,000) (9)	ε_{lat}^{80} (×1,000) (10)	μ (11)	Failure mode[d] (12)
S-1	EMACO patch/coating	150	50	—	267	6.09	2.2	3.8	1.05	2.7	1
S-2	Patch + 2 plies GFRP	150	54	—	1,016	48.7	24.1	26.1	25.8	7.0	4
S-3	2 plies GFRP	150	33	—	847	39.1	20.5	27.3	8.7	6.0	3
S-4	K-grout, 1-ply GFRP	200	83	—	1,151	31.7	4.6	10.2	25.8	5.5	3
S-5[b]	Expansive grout, 1-ply GFRP	200	78	27.5	864	22.5	4.13	10	2.8	3.8	2
S-6[b]	Expansive grout, 2 plies GFRP	200	96	50	1,283	36.0	9.26	15.5	5.3	4.5	2
S-7	Expansive grout, plastic tube + 2 plies GFRP	200	85	36	1,617	46.7	11.3	18	17.7	5.5	2
H-3a	1-ply GFRP	150	—	—	704	31.0	16.0	18.0	9.7	4.4	3
H-3	2 plies GFRP	150	—	—	1,125	55.0	26.3	30.0	12.3	4.8	4
H-5	Expansive grout, 1-ply GFRP	230	—	—	871	17.2	9.33	20	14	3.0	2
H-6	Expansive grout, 2 plies GFRP	230	—	—	1,437	30.9	24.6	29.3	10	4.6	4

[a]After 90 days of postrepair exposure to accelerated corrosion.
[b]These options include plastic foil for diffusion barrier between grout and GFRP.
[c]Measured core concrete stress.
[d]Failure modes: 1 = explosive, 2 = nominally ductile, 3 = ductile, 4 = very ductile.

specimen was then painted with a special water-based, alkali-resistant epoxy coating (trade name RJW 1000) which is meant to act as a barrier from further penetration of chlorides.

Option 2 is an extension of the traditional approach—two layers of glass fiber-reinforced plastic (GFRP) wrap were used on top of the EMACO/paint patch.

In Options 3–7, damaged concrete was no longer removed or replaced. Instead, after cleaning any staining and rust deposits from the specimen surface, the following alternatives were considered.

Option 3—The specimen surface was coated with alkali-resistant epoxy coating, and subsequently wrapped with two layers of glass fiber sheet.

Option 4—A 25 mm-thick layer of Type K grout was cast on the specimen surface (this increased the specimen diameter to 200 mm) followed by coating with alkali-resistant epoxy and one layer of glass fiber composite wrap.

Repair Options 5, 6, and 7 were designed to study the effect of active confining pressure. The composite wrap was prestressed by overlaying a 25 mm-thick layer of expansive grout on the surface of the specimen prior to wrapping. This type of grout develops 2.5% unrestrained expansion, and it is known to reach much higher levels of expansion under partially restrained conditions (Sheikh et al. 1994). Different numbers of layers of FRP wrap were used, i.e., one layer in Option 5 and two layers in Options 6 and 7.

For diffusion barrier (in order to seal out moisture and oxygen from the repaired specimen, and to protect the glass wrap from alkalis leaching out from the grout), a plastic foil was used directly on the grout surface (after the grout had set and prior to the application of the FRP wraps) in Options 5 and 6. A 3 mm-thick polypropylene sleeve was used as diffusion barrier under the wrap in repair Option 7. (Note that the same polypropylene sleeve was used as formwork for pouring the grout layer in all specimens of Options 4–7. This sleeve was relatively stiff in the lateral direction, providing partial restraint to grout expansion. The sleeve was removed a day later from specimens of Options 4–6 prior to application of the GFRP wrap as marked in Column (2) of Table 1.

After the first phase of accelerated corrosion most of the H-series specimens had disintegrated beyond repair. A total of 12 specimens survived into the last phase of the experimental program. Of those three were repaired as in Option 3 but using only one layer of composite wrap (referred to herein as Option 3a). Prior to wrapping, cracks and voids caused by spalled concrete were filled with EMACO grout to smoothen out the lateral surface of the specimen so as to avoid tearing off the wrap material. Repair Options 3, 5, and 6 (but without diffusion barrier) were tested on the remaining nine specimens (applied in groups of three specimens each). The forms used for pouring the expansive grout were very flexible laterally, and for this reason the diameter of the H-group of specimens of repair Options 5 and 6 had increased to 230 mm prior to application of the GFRP wrap a day later. This difference in the detail of grouting the S and H series of specimens appears important from some observed differences in performance. The repaired H-series specimens were only tested under mechanical load without further corrosion conditioning.

Properties of Repair Materials

FRP/GFRP Wrap

The product used in this study is the TYFO Fibrwrap System (HEXEL FYFE, Dublin, Calif.), which has been used in several repair projects in seismic and nonseismic applications. The material is a woven fabric containing E-glass fibers in the primary direction and orthogonally oriented Kevlar fibers; the fabric thickness is approximately 1.7 mm. It is provided in rolls and was easily formed as a wrap around the lateral surface of the specimens. To be applied on concrete the material must be first saturated in a special epoxy with high elongation characteristics which when eventually set and hardened provides the matrix for the fiber weave. After setting, the thickness of one composite layer is about 4 mm. In the primary fiber direction the composite has a specified minimum tensile strength of 420 MPa, tensile modulus of 21 GPa, and a corresponding maximum deformability at fracture of 2–4% (nominal properties supplied by the manufacturer; Isley 1992). Tensile strength in a direction orthogonal to the primary fibers is 33.1 MPa. An overlap of at least 100 mm is necessary to ensure that the wrap can develop its tensile capacity. The composite is resistant to corrosive agents such as salt and soil, and sustains its mechanical properties over time in low and high temperatures. It is also sensitive to UV radiation.

Type K Grout

This is shrinkage compensating cement. The composition of the mix used was $w_0 = 0.53$, Type K cement:sand ratio 1:2 by weight.

Expansive Grout

Expansive grout develops expansion due to formation of ettringite (Sheikh et al. (1994). The composition of the mix used was 60% (by weight) portland cement Type 10, 25% high alumina cement, 12% plaster of paris, 3% hydrated lime, superplasticizer (312 g/100 kg of portland cement), and w_0 of 0.4.

POSTREPAIR RESPONSE TO ACCELERATED CORROSION

After the repairs, the S-series specimens were subjected to a second phase of accelerated corrosion following the same procedures as described in the preceding section. Electrical current and radial expansion strains were continuously monitored to assess the influence of the various repair methods on the resulting corrosion rate. Table 1 outlines the repair option used, the associated specimen identification, and the most important measured indices of postrepair response to accelerated corrosion and mechanical testing. Fig. 5(a) plots radial expansion time histories for some of the repaired specimens whereas cumulative steel loss versus time is plotted in Fig. 5(b). Each curve is the average of three specimens. As in the prerepair stage it appears that radial expansion correlates with the amount of steel loss; options causing the least amount of expansion are those with the correspondingly lower amounts of steel loss, i.e., more resistant to current flow. It is interesting to note that the options with a diffusion barrier demonstrated higher loss of steel section, indicating their resistivity was lower than that of the other repaired specimens. It appears that moisture entrapped during casting of the external grout layer could not easily dry because both the GFRP jacket and the diffusion barrier sealed the specimen, thus eliminating the

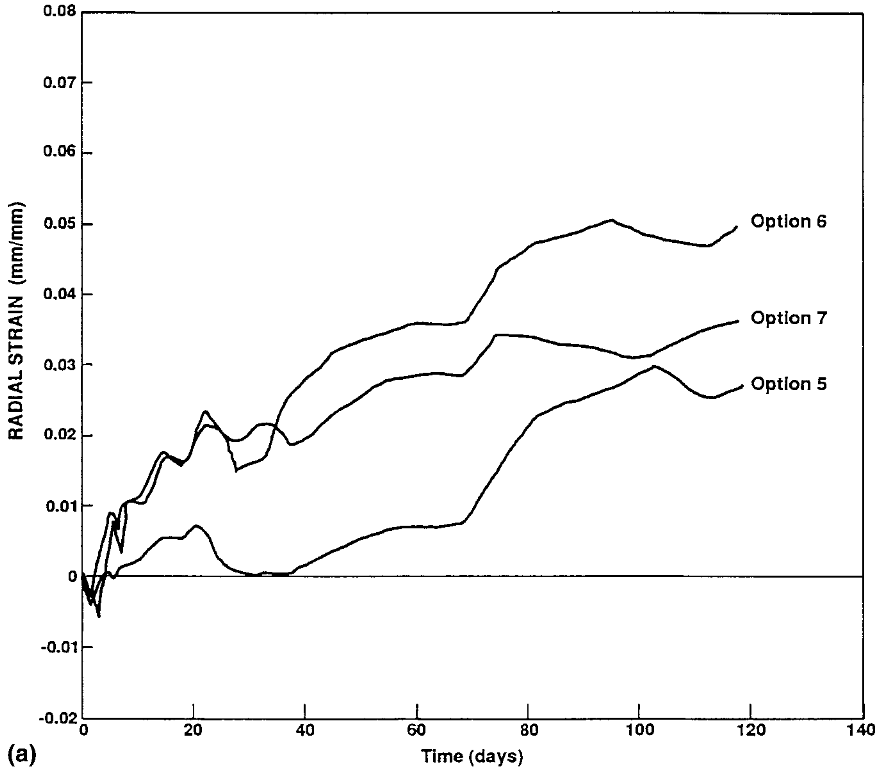

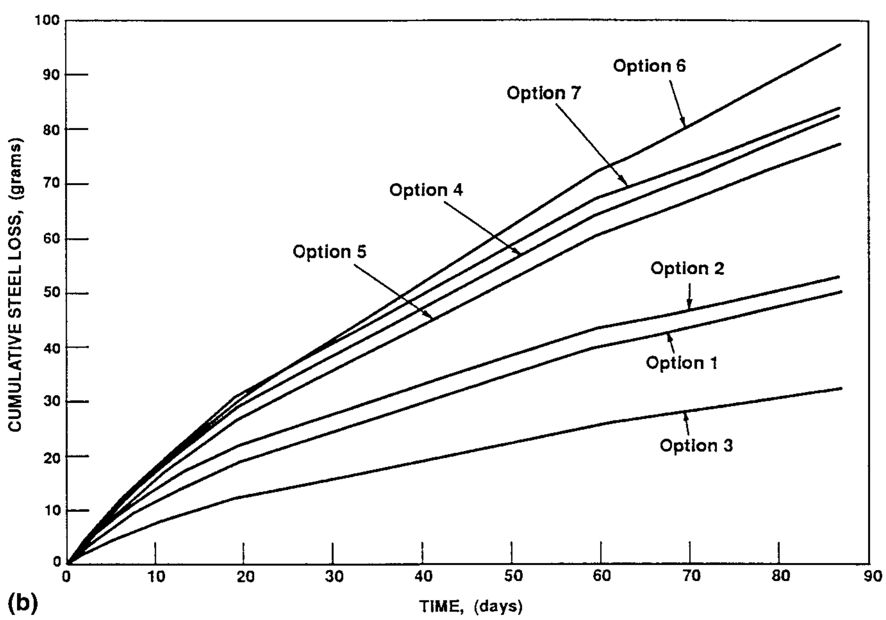

FIG. 5. Postrepair Performance of Specimens in Accelerated Corrosion Conditions: (a) Radial Expansion Strains versus Time; (b) Estimated Cumulative Steel Loss versus Time

main route for convective activity. (Note that prior to grouting specimens had been stored in a dry environment for several months.) Because of the resulting higher degree of saturation, specimens repaired with Options 4–7 were more conductive to electrical current; to eliminate this pitfall, the grout should be left to dry thoroughly before use of GFRP jacketing.

PERFORMANCE UNDER MECHANICAL LOAD

The last stage of the experimental program was testing of the specimens under concentric compression to failure. Figs. 6(a) and 7(a) plot representative samples of axial stress versus axial strain histories for the S and H series of repaired specimens, respectively. Lateral strain was also recorded on the specimen surface; the experimental values are plotted against the imposed axial strain in Figs. 6(b) and 7(b) for representative samples of the two repaired-specimen groups. Average values for the peak compressive load, the corresponding axial strain ε_{peak}, and the axial and lateral strains ε_{80} and ε_{lat}^{80}, respectively, corresponding to postpeak load equal to 80% of the peak value are listed in Table 1 for all repair options. Deformation ductility μ was calculated from the ratio $\varepsilon_{80}/\varepsilon_y$, where ε_y is the strain corresponding to the point of change of the initial stiffness in the load-deformation curve of the member. The force taken by the concrete part of the cross section was determined from the difference between the total load and the nominal load carried by the longitudinal reinforcement (=4 $\times$ 100 mm^2 $\times$ 400 MPa). For specimens jacketed with FRP wraps the core concrete stress was obtained by dividing the concrete force by the total encased area, whereas for repairs not using FRP jacketing the core area used in this calculation was defined as the part of the cross section enclosed by the transverse spiral reinforcement. (In calculating the axial stress the change in the nominal specimen diameter incurred by the repair was considered as listed in Table 1.) It is debatable whether the longitudinal reinforcement continues to sustain its full yield capacity when the reinforcement cage is as damaged by corrosion as in this series of specimens. With the degree of section loss and embrittlement that the stirrups had sustained, they could not effectively support the longitudinal reinforcement against lateral buckling, unless the repair scheme used included stiff confining jackets. (Note, for example, the premature failure of the S-1 group of specimens at a load much lower than would correspond to the unconfined compressive strength of the core concrete.) Thus, the stress calculation in Table 1 underestimates more the stress carried by concrete in repairs that had little or no GFRP jackets.

The level of the confining pressure applied by the GFRP jacket is $\sigma_{lat} = 2F/D$, where F is the force in the jacket and D is the specimen diameter; $F = E^{GFRP}\varepsilon_{lat}t_{ply}$, where E^{GFRP} is the elastic modulus of the jacketing composite and t is the thickness of the jacket (= number of plies $\times$ thickness of one ply), therefore $\sigma_{lat} = 2E^{GFRP}\varepsilon_{lat}t_{ply}/D$. Considering that a single ply thickness is about 1.7 mm, and E^{GFRP} = 21 GPa, it follows that $\sigma_{lat} = nK\varepsilon_{lat}$, where n is the number of layers and K = 476, 357, and 310 for the three diameters used in Table 1. The average confining stresses at 80% of the peak load (near or at failure) were calculated from the measured strain values, as listed in Table 2. Note that where measured, the expansion strains due to postrepair corrosion which preceded application of the mechanical load (S-series of specimens) indicate the existence of preconfinement on the lateral surface of the specimen. However, because these strain values built up gradually over a period of 90 days (prior to loading the specimens), they were subject to creep of the GFRP wrap, and hence, using them directly in the above calculation would tend to overestimate the true confining pressure. Probably the most important effect of prestressing the wrap, either by means of expansive grout, or by the expansive tendency of the embedded corroding reinforcement, is to reduce the available strain capacity of the wrap material in the hoop direction, which is represented by the ε_{lat}^{80} value in Table 1. This explains why specimens repaired by Options 5 or 6 which included expansive grout with no other restraining mechanism failed at very low lateral strains. Option 6 having two layers of GFRP jacket performed better than Option 5. Option 4 which included K-grout with

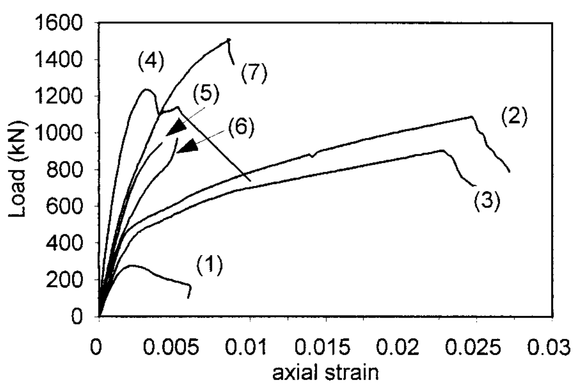

FIG. 6(a). Axial Load versus Axial Strain Diagram for Repaired S-Series Specimens

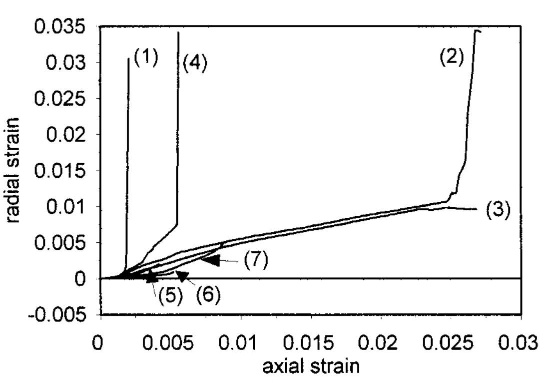

FIG. 6(b). Radial Strain versus Axial Strain Diagram for Repaired S-Series Specimens

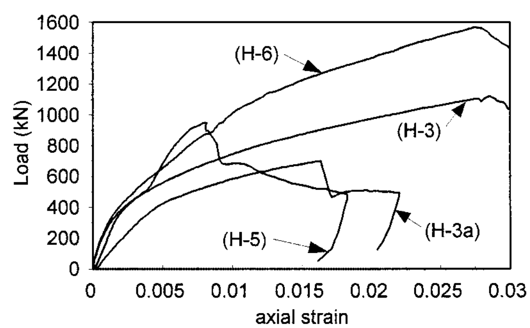

FIG. 7(a). Axial Load versus Axial Strain Diagram for Repaired H-Series Specimens

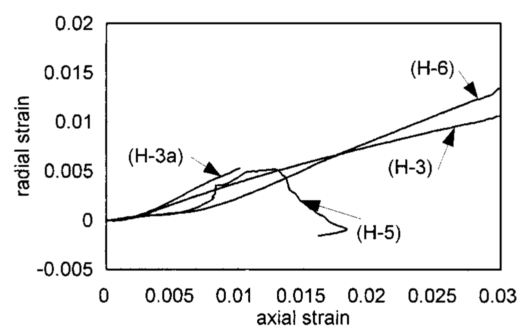

FIG. 7(b). Radial Strain versus Axial Strain Diagram for Repaired H-Series Specimens

TABLE 2. Estimated Confining Pressure near Failure (f_{cc} = Confined Strength; f_c = 24 MPa)

Specimen (1)	n plies (2)	K (3)	ε_{lat}^{80} (4)	σ_{lat} (5)	$\lambda = (f_{cc} - f_c)/\sigma_{lat}$ (6)
S-1	0	476	0.0011	0.0	<0
S-2	2	476	0.0258	24.5	1.0
S-3	2	476	0.0087	8.3	1.8
S-4	1	357	0.0258	9.2	0.83
S-5	1	357	0.0028	1.0	<0
S-6	2	357	0.0053	3.78	3.17
S-7	2	357	0.0177	12.6	1.8
H-3a	1	476	0.0097	4.62	1.5
H-3	2	476	0.0123	11.7	2.65
H-5	1	310	0.0140	4.35	<0
H-6	2	310	0.0100	6.2	1.1

very low expansion characteristics and a single ply of GFRP wrap performed much better than Option 5 which had the same details except in the expansion properties of the grout.

The ratio $(f_{cc} - f_c)/\sigma_{lat}$ is motivated by the familiar results of conventional confinement according to which the confined compressive strength of concrete f_{cc} is increased over the unconfined value f_c by an amount proportional to the lateral stress σ_{lat}: $f_{cc} = f_c + \lambda\sigma_{lat}$. The significance of the result $\lambda < 0$ is that premature failure occurred in the system by some mechanism other than concrete crushing, e.g., delamination of the wrap, anchorage failure of the ply overlap, rupture of corroded stirrups, and tearing of the wrap by breakage of the plastic sleeve. The maximum reported values for λ were 3.17 (Option S-6) and 2.65 (Option H-3). The two groups are differentiated because it is plausible that the spiral steel in the S-series provided some degree of confining action despite its poor and embrittled condition. The λ values are somewhat lower than what is observed when spiral steel reinforcement is used for confinement (=4.1 as per Richart's original equation $f_{cc} = f_c + 4.1\sigma_{lat}$). Obviously λ depends on the axial stiffness of the jacket; other studies on the efficacy of FRP wraps in strengthening concrete have also yielded values for λ around 3 (Lee 1998).

Jacketing with GFRP wraps was an effective means to recover strength and supply ductility in all cases studied. The repair Option 2 (EMACO grout with two plies of GFRP wrap) was the most successful solution in all aspects considered, i.e., postrepair steel loss was minimal, strength gain was substantial, and response to mechanical load very ductile. Option 3 also performed very well, following closely the results of Option 2. This result is of great practical significance, because Option 3 is the least expensive, easier to implement, repair scheme. The worst response was displayed by Option 1 which is the conventional repair option most commonly used in practice. Using expansive grouts (Options 5 and 6) did not prove an effective alternative in raising any of the significant performance variables, particularly so in comparison with the plainer Option 3. Option 4 with K-grout and a single ply of GFRP wrap was adequate in terms of strength and ductility increase and was much preferable over Option 5, but is considered inferior to Option 3, particularly when considering the increased labor effort associated with its implementation. In terms of mechanical properties Option 7 which contained an additional restraining mechanism (3 mm-thick polypropylene sleeve) was very effective in raising the strength of the specimen, but failure was nominally ductile resulting from sudden fracture of the sleeve. For this reason and also because of the bad performance of this method in slowing down corrosion, Option 7 is not a recommended practical alternative for repair of corroded reinforced concrete elements.

Whereas the S-series of specimens were subjected to postrepair-accelerated corrosion which caused some degree of pretensioning to the GFRP wraps after placement even in the absence of expansive grout, the H-series of specimens were inert from the time of repair to the time of mechanical load testing. For this reason, the H-series of repaired specimens performed generally better than similarly repaired specimens from the S-series. For example, the H-3 specimens (repaired with two plies of GFRP wrap) reached the highest strength and deformation capacity from among all repaired groups. Option 3a with one ply of GFRP wrap was also successful; the observed strength increase was similar to that of the S-4 option (K-grout and 1-ply GFRP wrap), but the deformation capacity of specimens H-3a was much greater, most likely because the wrap in the S-4 series was partially prestressed by expansive corrosion products that had accumulated after the repair. As in the S-series, prestressing the wrap even further by injection of an expansive grout layer did not improve the response as was initially anticipated in designing the repair. By reducing the available deformation capacity either of the wrap itself or of the anchorage zone, expansive grout accelerates the repair failure at lower deformation level and with a more brittle mode of failure.

CONCLUSIONS

This paper explored the performance and efficiency of jacketing with FRP wraps as an alternative to conventional repair methods for corrosion-damaged reinforced concrete columns. For this purpose an extensive experimental parameter study was conducted on several small-scale concrete columns with various reinforcement configurations. To simulate natural corrosion damage the specimens were subjected electrochemically to accelerated corrosion conditions in the laboratory. The expansive forces generated by accumulating corrosion products around the main reinforcement caused severe damage to the specimens particularly in cases with marginal confining steel. The motivating premise of all the repair options considered was that external confinement in the form of jacketing could alter favorably the process of corrosion by slowing down the rate of the corrosion reaction, and imparting ductility and strength to the affected structural element. FRP wraps, being strong and corrosion-resistant, proved very effective as jacketing material. Compared with the conventional repair methods which consist primarily of removing the contaminated concrete cover and replacing with low permeability patch, practically all the alternatives considered performed much better in terms of strength and durability. Performance was markedly improved when increasing the number of FRP layers used in the jacket. A critical detail for the success of the repair was providing sufficient anchorage to each wrap layer by overlapping the ends. Prestressing the wrap by injecting expansive grouts between the jacket and the specimen did not improve the performance of the repair. Rather, after setting, the composite jacket became rather impermeable, resulting in concentration of entrapped moisture in the grout layer, thereby promoting the corrosion rate by lowering the resistivity of the entire column-jacket system. Furthermore, the available deformation capacity of the jacket was reduced by the expansive forces generated by the grout, and therefore mechanical properties of the repaired system such as strength recovery and deformation capacity were compromised rather than improved by this alternative. The repair option that performed best with regard to the postrepair corrosion rate, strength recovery, and deformation capacity was also the simplest and easiest to implement alternative, consisting of cleaning the damaged surface (but without removal of contaminated or cracked cover concrete) and wrapping directly on layers of fiber-reinforced composite wraps. Testing the performance of FRP-jacketed corroded members of rectangular cross sections, and consideration of combined flexure/axial load action in assessing the effectiveness of the repair schemes would be necessary prior to recommending general implementation of this technology to field applications.

ACKNOWLEDGMENTS

Primary funding for the experimental program presented in this paper was provided by the Ministry of Transportation of Ontario during the period 1995–1996. Repair materials were provided by R. J. Watson, Inc. (Bridges and Structural-Engineered Systems, East Amherst, N.Y.).

APPENDIX I. REFERENCES

Bonacci, J. F., et al. (1998). ''Laboratory simulations of corrosion in reinforced concrete and repair with CFRP wraps.'' *Proc., CSCE 1998 Annu. Structural Specialty Conf.*, J. P. Newhook and L. G. Jaeger, eds., CSCE, Montreal, 653–662.

Isley, F. (1992). ''TYFO S epoxy and TYFO SEH-51 composite.'' *Res. and Devel. Lab. Rep.*, HEXCEL FYFE Associates, Dublin, Calif.

Lee, C. (1998). ''Accelerated corrosion and repair of reinforced concrete columns using CFRP sheets.'' MASc thesis, Dept. of Civ. Engrg., University of Toronto.

Manning, D. G. (1992). *The design life of structures*, ''Design life of concrete highway structures—The North American scene.'' Blackie and Son, Ltd., London, 144–153.

Michniewicz, J. (1996). ''Repair and rehabilitation of reinforced concrete columns with fibre-reinforced plastics.'' MEng thesis, Dept. of Civ. Engrg., University of Toronto.

Pantazopoulou, S. J., Bonacci, J. F., Hearn, N., Sheikh, S. A., and Thomas, M. D. A. (1996). ''Repair of corrosion damaged concrete using advanced composite materials.'' *Proc., 2nd Int. on Advanced Compos. Mat. in Bridges and Struct. Conf.*, Canadian Society for Civil Engineering, Montreal, 457–463.

Phillips, J. (1992). ''The effect of corrosion on the structural performance of new and repaired one-way slabs.'' PhD thesis, Dept. of Civ. Engrg., University of Toronto.

Sheikh, S., Pantazopoulou, S., Bonacci, J., Thomas, M., and Hearn, N. (1997). ''Repair of delaminated circular pier columns by ACM.'' *Ontario Joint Transp. Res. Rep. No. 31902*, Ministry of Transportation of Ontario, Canada.

Sheikh, S. A., Fu, Y., and O'Neill, M. W. (1994). ''Expansive cement concrete for drilled shafts.'' *ACI Mat. J.*, 91(3), 237–245.

APPENDIX II. NOTATION

The following symbols are used in this paper:

E^{GFRP} = modulus of elasticity of jacketing material in primary direction (hoop);
f_c = unconfined cylinder compressive strength;
f_{cc} = confined concrete compressive strength;
I = corrosion current (A);
K = jacket layer stiffness;
n = number of jacketing plies;
t = time of active corrosion since initiation (s);
t_{ply} = thickness of single ply;
ε_{lat} = lateral (hoop) strain;
ε_{lat}^{80} = lateral strain at postpeak load corresponding to 80% of peak load;
ε_{80} = axial compressive strain at postpeak load corresponding to 80% of peak load;
λ = confinement coefficient; and
σ_{lat} = lateral confining pressure.